

Electrical and Optical Properties of Carbon Nanotube Hybrid Zinc Oxide Nanocomposites Prepared by Ball Mill Technique

Ömer Guler, Seval Hale Guler, Fahrettin Yo, Handan Aydin, Cihat Aydin, Farid El-Tantawy, El-Shazly M. Duraia & A. N. Fouda

To cite this article: Ömer Guler, Seval Hale Guler, Fahrettin Yo, Handan Aydin, Cihat Aydin, Farid El-Tantawy, El-Shazly M. Duraia & A. N. Fouda (2015) Electrical and Optical Properties of Carbon Nanotube Hybrid Zinc Oxide Nanocomposites Prepared by Ball Mill Technique, Fullerenes, Nanotubes and Carbon Nanostructures, 23:10, 865-869, DOI: [10.1080/1536383X.2015.1022256](https://doi.org/10.1080/1536383X.2015.1022256)

To link to this article: <http://dx.doi.org/10.1080/1536383X.2015.1022256>



Accepted author version posted online: 18 May 2015.



Submit your article to this journal [↗](#)



Article views: 68



View related articles [↗](#)



View Crossmark data [↗](#)

Electrical and Optical Properties of Carbon Nanotube Hybrid Zinc Oxide Nanocomposites Prepared by Ball Mill Technique

ÖMER GULER¹, SEVAL HALE GULER¹, FAHRETTIN YO², HANDAN AYDIN², CIHAT AYDIN³, FARID EL-TANTAWY⁴, EL-SHAZLY M. DURAIA⁴, and A. N. FOU DA⁴

¹Department of Metallurgical and Materials Science, Engineering Faculty, Firat University, Elazig 23119, Turkey

²Department of Physics, Faculty of Science, Firat University, Elazig 23119, Turkey

³Department of Metallurgical and Materials Science, Technology Faculty, Firat University, Elazig 23119, Turkey

⁴Department of Physics, Faculty of Science, Suez Canal University, Ismailia, Egypt

Received 4 January 2015; accepted 19 February 2015

The electrical and optical properties of carbon nanotubes hybrid zinc oxide (ZnO-CNTs) nanocomposites synthesized by ball mill technique have been investigated. The nanocomposites were prepared using zinc oxide (ZnO) powder and carbon nanotube (CNT) synthesized by catalytic thermal chemical vapor deposition (CVD). The diameters and lengths of the CNTs were respectively determined to be 20–30 nm and about 3–5 μm . DC conductivity measurements reveal that the nanocomposites are good conductive material. The room temperature DC electrical conductivity σ_{dc} of the un-doped ZnO and ZnO-CNT nanocomposites with 0.1% CNT, 0.5% CNT, and 1% CNT were found to be 6.55×10^{-5} , 5.46×10^{-4} , 1.49×10^{-3} , and 4.01×10^{-3} S/cm, respectively. This indicates that there is a remarkable improvement of the electrical conductivity as the CNTs' content increases. The optical band gaps of the composites were determined by Kubelka-Munk theory based on the analysis of diffuse reflectance. The band gap (E_g) values of the composites decreased with increasing CNT contents. The obtained results indicate that the electrical and optical properties of ZnO semiconductor can be improved by incorporation of CNT.

Keywords: ZnO-CNTs hybrid, microstructure, electrical conductivity, optical properties

Introduction

Zinc oxide (ZnO) is one of the promising wide band gap (E_g) semiconductors with E_g of 3.37 eV and a large exciton binding energy of 60 meV, which is efficient in opto-electronic devices. In addition, it has potentially useful properties including low cost in production, commercial availability, piezoelectricity, catalytic activity, chemical stability, and biocompatibility. Economically, it has various applications as a luminescent material, photodiode, dye-sensitized solar cells, gas sensing, photo-catalyst, antibacterial, and more (1–5).

Hybrids of carbon nanotubes (CNTs) with inorganic materials have attracted much attention due to their potential application as photo-catalyst, gas sensors, supercapacitors, and field-emission devices (7). Zinc oxide and multiwalled carbon nanotubes (ZnO-MWCNTs) represent one of the most important members of the MWCNT-inorganic composites groups. The ZnO-MWCNT composites have been

prepared by various methods and their properties are different from MWCNT and ZnO alone (6–8).

In the present study, improvement in the electrical and optical properties of zinc oxide-carbon nanotube nanocomposites has been achieved. The enhancement in the electrical and optical properties of zinc oxide-carbon nanotube nanocomposites was attributed to the variation of the microstructure.

Experimental Details

Commercial ZnO powders (purity: 99.5%) with particle size of 10 μm were used for preparation of the composites. *P*-type Si (100) substrates were used to grow the CNTs. Firstly, the substrates were rinsed consecutively in acetone and ethanol in an ultrasonic bath. After cleaning, thin Ni layer (20 nm) was deposited over the silicon substrates in order to catalyze the CNTs' growth. The substrates were placed in the center of quartz tube reactor in the tube furnace. The tube was evacuated and the pressure was kept at 10^{-3} Torr. The furnace was heated to 450°C and kept at this temperature for 40 min in order to break the continuous layer of the Ni catalyst into nano-islands that are suitable for the CNTs' growth. Then, the furnace was heated to 650°C under Ar gas atmosphere (1 L/min) at 2 Torr and then, the C_2H_2 gas was flushed for

Address correspondence to A. N. Fou da or Farid El-Tantawy, Department of Physics, Faculty of Science, Suez Canal University, Ismailia, Egypt. E-mail: alynabieh@yahoo.com; faridtantawy@yahoo.com

Color versions of one or more figures in this article can be found online at www.tandfonline.com/lfnn.

another 40 min. Finally, the furnace was naturally cooled in Ar atmosphere. The sample color was completely changed into black indicating the formation of the CNTs. The prepared CNTs were scratched from the surface and collected for the composite preparation.

The carbon nanotubes hybrid zinc oxide (ZnO-CNTs) composites prepared for the ratios of the carbon nanotubes: ZnO are 0.1%, 0.5%, and 1%. In order to disperse the CNTs homogeneously in the matrix, the CNTs were weighed at appropriate ratios and then added to 50 ml volume of ethanol followed by mild sonication for 1 hr in order to avoid nanotube agglomeration. Then, ZnO powders were added to the mixtures and the mixtures were stirred via magnetic stirrer at 80°C until the alcohol was evaporated. The obtained powders were milled for 1 hr at 300 rpm under argon atmosphere in a planetary ball mill. Retsch PM 100 branded mill system was used. During milling, 8 mm diameter steel balls were used and an effective dispersion was obtained. Ball milled powder mix was compacted in a 20 mm diameter compaction die at 600 MPa. The compacted powder was sintered at 600°C for 1 hr in Ar ambient.

The CNTs obtained were characterized via XRD (Bruker Advance D8, CuK α) diffraction and HR-TEM (Jeol Jem 2100F) techniques. The composites were analyzed by FESEM (Jeol Jsm-7001F). Electrical conductivity of the composites was measured using two-probe method with the help of Keithley 6517A Electrometer/High-Resistance Meter. Optical measurements of the samples were performed using a Shimadzu UV- VIS 3600 spectrophotometer.

Results and Discussion

Structural Observation of CNT/ZnO Nanocomposites

Figure 1 (a and b) shows HR-TEM images of CNT/ZnO nanocomposites. As seen in HR-TEM images, the dense tangled CNTs were observed. The diameters and lengths of the CNTs were determined to be 20–30 nm and about 3–5 μm , respectively. It was noticed that the diameter of the CNTs is very close to the thickness of the nickel catalyst. This result supports the fact that the diameter of the CNTs can be predetermined by the size of the catalyst nanoparticles (9–12). It is clear from the figure that the CNTs are not well aligned but have a spaghetti morphology. The surface of the CNTs was found to be clean since there is no amorphous carbon and other graphitic structures were not observed to be attached to the surface of the CNTs. This confirms the quality of the prepared CNTs. The surface morphology of the synthesized composites was identified by SEM measurements. As seen in Figure 2, in 0.1% CNTs reinforced sample, the CNTs were randomly distributed. This can be attributed to the relatively small amount of CNTs. In addition, CNTs were homogeneously distributed in the matrix. The CNTs were completely dissolved when the doping percentage was 0.1%. But, in the case of 0.5% and 1% doping, the dissolving of CNT and dispersion of CNTs in the matrix were relatively limited. In 1% CNT reinforced composite, the CNTs were wrapped up like a cobweb on ZnO grains. In certain regions, no CNTs'

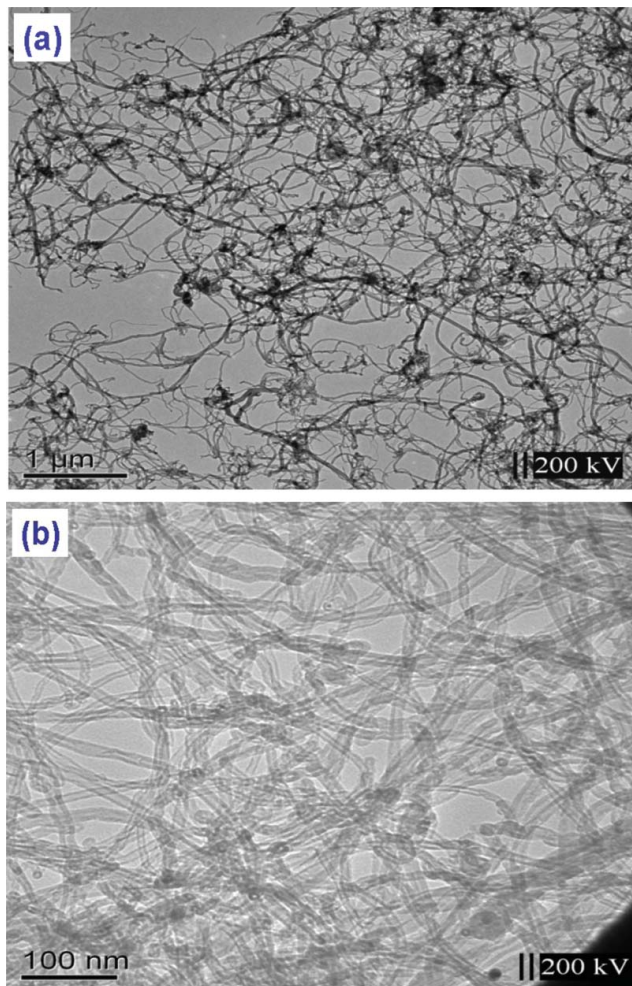


Fig. 1. (a,b). HRTEM images of as synthesized carbon nanotubes (CNT) via CVD method with different magnification: (a) 1000 \times and (b) 10,000 \times .

bundles were dissolved and they remain as cluster or aggregates. In the composites, the length of the CNTs was shortened. This resulted from the applied ball milling order and mild sonication. As seen from these images, the homogeneous distribution in composite of CNTs was increasingly difficult with the increase in the CNTs' quantity of composites.

Electrical Conductivity Measurements

The electrical transport mechanisms of CNTs-ZnO nanocomposites were studied as a function of temperature, as seen in Figure 3. It has been found that the electrical conductivity of the composites increases with increasing temperature. The conductivity curves can be analyzed using the following relation (9–10):

$$\sigma_{dc} = \sigma_0 \exp\left(-\frac{E_a}{KT}\right) \quad (1)$$

Where σ_0 is the pre-exponential factor, k is the Boltzmann's constant, and E_a is the activation energy. E_a values were calculated from the slope of the linear portions of Figure 3 and

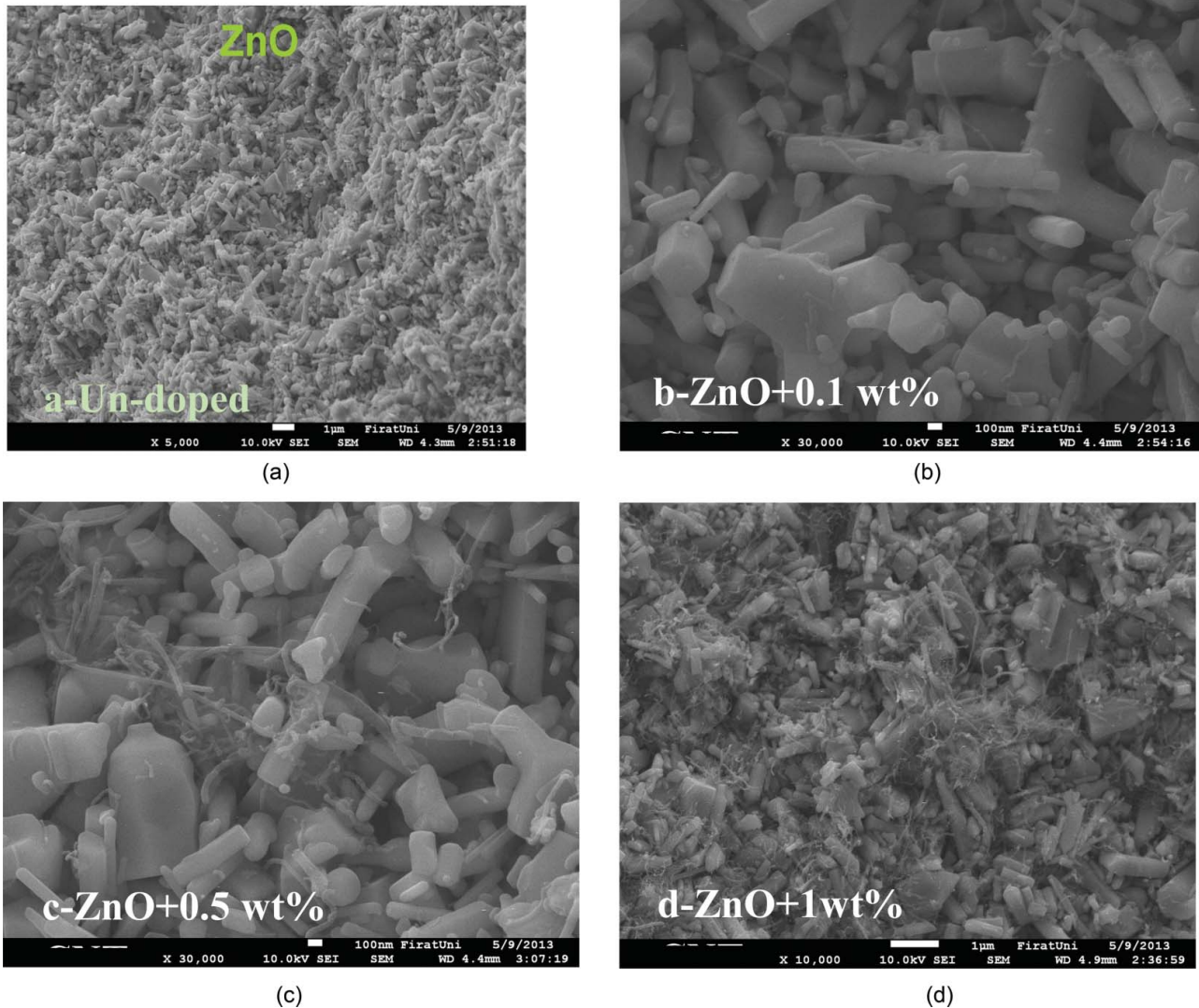


Fig. 2. (a–d). SEM images of the composites (a) undoped ZnO, (b) 0.1wt% CNT, (c) 0.5wt% CNT, and (d) 1wt% CNT.

are given in Table 1. E_a values of the nanocomposites did not show a regular trend with increasing CNTs' content. This is due to the non-uniform distribution of CNTs into ZnO host matrix. The composite with 0.5% CNTs exhibits the lowest activation energy, whereas the highest activation energy was found to be for the composite with 0.1% CNT. The room temperature conductivity σ_{25} values of the un-doped ZnO, 0.1% CNT, 0.5% CNT, and 1% CNT were found to be 6.55×10^{-5} , 5.46×10^{-4} , 1.49×10^{-3} , and 4.01×10^{-3} S/cm, respectively. The conductivity is getting higher with increasing CNTs' content. The CNT provides additional conduction paths in the nanocomposite and in turn, the conductivity is increased. As the temperature increases, more charge carriers overcome the activation energy barrier in the composites and the elevated temperatures cause an increase in number of charge carriers participating in the electrical conduction. Under ambient conditions, due to the coverage of CNTs by oxygen, it behaves like a *p*-type semiconductor (15). On the other hand, ZnO is an *n*-type semiconductor due to native

defects. In the case of partially covered CNTs with ZnO nanoparticles, the majority carriers of ZnO-CNTs are holes. In contrast, when CNTs are completely covered with ZnO nanoparticles, the majority carriers of the ZnO-CNT are electrons. This can be attributed to the transfer of charge from ZnO to CNTs and the composites behave like *n*-type semiconductor (16). The migration of electrons from the conduction band of ZnO to CNTs is related to the strong interfacial connection between CNTs and ZnO (17).

CNTs are considered as one of the nearly perfect conductors at room temperature (18). For this reason, the conductivity of the materials increases with CNTs' contents. Sun Park et al. revealed that enhancement of electron mobility is five-fold for ZnO/N-CNTs nanocomposite transport layer with 0.08wt% CNT (19). It is known that the electrical properties of CNTs and graphene are quite similar. Khurana et al. revealed that the electron transfer kinetics are faster in ZnO-graphene composite than ZnO. Faster charge transfer is attributed to the presence of graphene (20). In addition,

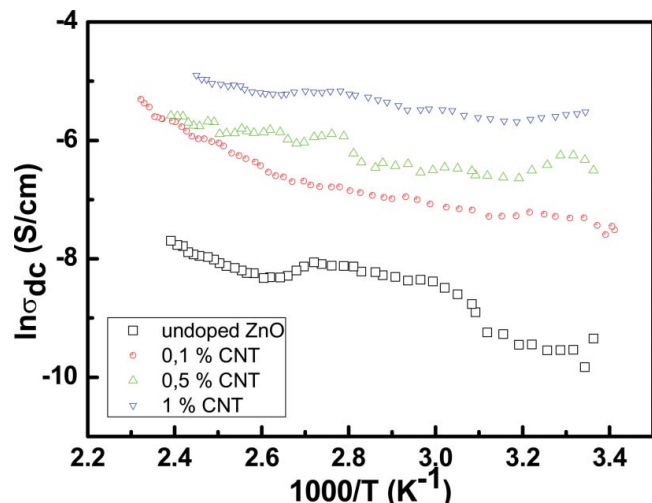


Fig. 3. Plots of the electrical conductivity versus temperature of the studied nanocomposites.

Sarkar et al. showed in their study that the electrical conductivity of Al_2O_3 -CNT composite was increased by increasing the quantity of CNTs (21).

Optical Properties of the CNTs-ZnO Nanocomposites

Figure 4 represents the plots of the diffused reflectance for un-doped and CNTs-doped ZnO nanocomposites. The reflectance of the composites indicates a sharp increase at 370 nm. The reflectance of the composites is decreased with CNTs' contents. The decrease in reflectance is due to the increase in absorbance of the nanocomposites. Moreover, the change in reflectance of the samples with CNT dopants results from the surface and the internal reflection effects of the composites, because the CNT dopants change the color and surface properties of the composites and in turn, the absorption of the samples is increased and thus, the reflectance is decreased with CNTs' level.

The optical band gaps of the composites were determined using Kubelka-Munk theory for the analysis of diffuse reflectance spectra obtained from weakly absorbing samples. The reflectance spectra of the nanocomposites indicate that they are softly absorbing materials. Kubelka-Munk function can be determined by the following relation (22–26).

$$F(R) = \frac{(1-R)^2}{2R} \quad (2)$$

Table 1. The electronic parameters of the composites

Samples	E_a (eV)	σ_{dc} (S/cm)
Un-doped ZnO	0.144	6.55×10^{-3}
0.1% CNT-doped ZnO	0.085	5.46×10^{-4}
0.5% CNT-doped ZnO	0.068	1.49×10^{-3}
1% CNT-doped ZnO	0.083	4.01×10^{-3}

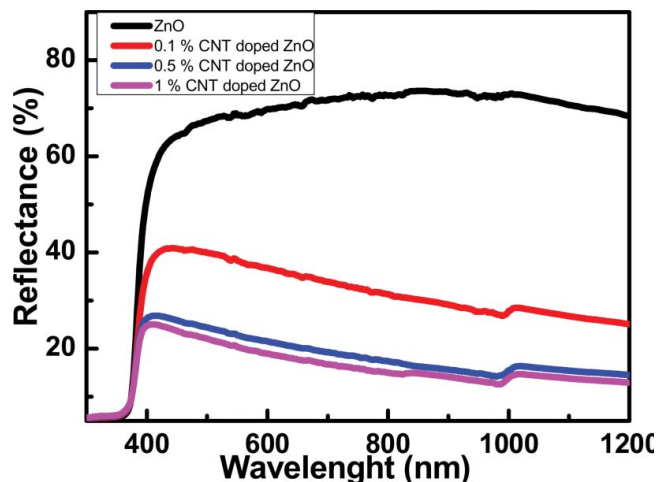


Fig. 4. Plots of the electrical conductivity versus temperature of CNT/ZnO nanocomposites.

Where R is the reflectance, and $F(R)$ is the Kubelka-Munk function corresponding to absorbance. Optical band gap can be calculated from the reflectance measurements by applying the Kubelka-Munk function (26). Thus, the conventional semiconductors relation that is used to determine the optical band gap can be rewritten as:

$$F(R)hv = A(hv - E_g)^n \quad (3)$$

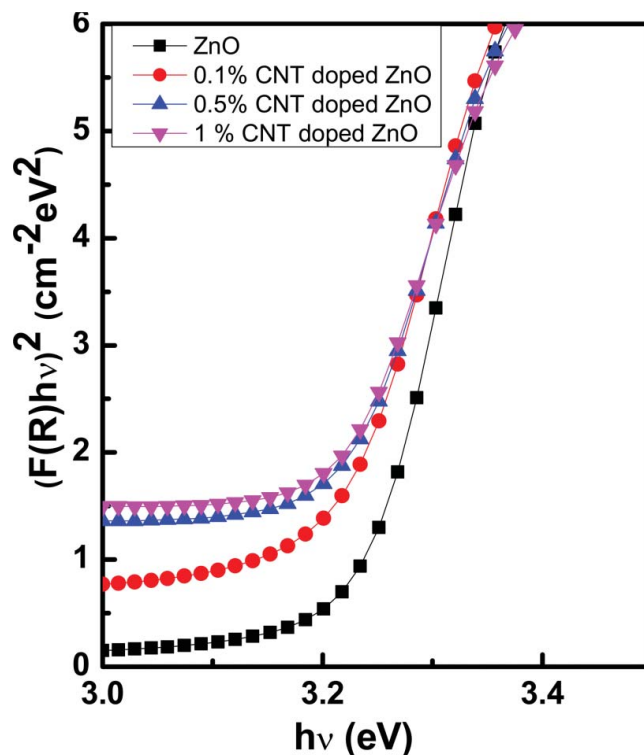


Fig. 5. Plots of $(F(R)hv)^2$ versus the photon energy (hv) of the CNT/ZnO nanocomposites.

Table 2. Optical band gap values of the composites

Sample	E_g (eV)
Un-doped ZnO	3.26
0.1% CNT-doped ZnO	3.24
0.5% CNT-doped ZnO	3.23
1% CNT-doped ZnO	3.22

Where E_g is the optical band gap, A is a constant, and n is a constant exponent that determines the type of optical transitions. For direct allowed transition, $n = 1/2$. The optical band gap of the composites was determined from the plots of $(F(R)h\nu)^2$ versus $h\nu$, as shown in Figure 5 and given in Table 2. The obtained E_g value of ZnO is in agreement with the other studies (27–29). As seen in Table 2, the E_g values of the nanocomposites are decreased with increasing CNTs' content. The electronic bands are expanded with CNTs' incorporation to ZnO and in turn, the optical band gap is decreased with CNTs' contents.

Conclusion

ZnO-CNT nanocomposite has been successfully prepared by ball mill technique. Electrical and optical properties of the prepared composite have been investigated. The increase in DC conductivity indicates that the nanocomposite is also a good conductive material, satisfying Mott's variable range hopping model for a two-dimensional conduction. Such nanocomposite may find extensive application in dye-sensitized solar cells, sensors, and supercapacitors.

References

- Wang, C. Y. and Adhikari, S. (2011) ZnO-CNT composite nanotubes as nanoresonators. *Phys. Lett. A*, 375: 2171–2175.
- Wang, Z. L. (2008) Splendid one-dimensional nanostructures of zinc oxide: A new nanomaterial family for nanotechnology. *ACS Nano*, 2: 1987–1992.
- Liangyuan, C., Zhiyong, L., Shouli, B., Kewei, Z., Dianqing, L., Aifan, C., and Chiu Liu, C. (2010) Synthesis of 1-dimensional ZnO and its sensing property for CO. *Sens. Actuators B*, 143: 620–628.
- Krunks, M., Katerski, A., Dedova, T., and Oja Acik, I. (2008) Nanostructured solar cell based on spray pyrolysis deposited ZnO nanorod array. *Solar Energy Mater. Sol. Cells*, 92: 1016–1019.
- Kou, J., Li, Z., Guo, Y., Gao, J., Yang, M., and Zou, Z. (2010) Photocatalytic degradation of polycyclic aromatic hydrocarbons in GaN: ZnO solid solution-assisted process: Direct hole oxidation mechanism. *J. Mol. Catal. A*, 325: 48–54.
- Samadi, M., Shivaeae, H. A., Zanetti, M., Pourjavadi, A., and Moshfegh, A. (2012) Visible light photocatalytic activity of novel MWCNT-doped ZnO electrospun nanofibers. *J. Mol. Catal. A Chem.*, 359: 42–48.
- Eder, D. (2010) Carbon nanotube-inorganic hybrids. *Chem. Rev.*, 110: 1348–1385.
- Chrissanthopoulos, A., Baskoutas, S., Bouropoulos, N., Dracopoulos, V., Tasis, D., and Yannopoulos, S. N. (2007) Novel ZnO nanostructures grown on carbon nanotubes by thermal evaporation. *Thin Solid Films*, 515: 8524–8528.
- Duraia, E.-S. M. A., Hannora, A., Mansurov, Z. A., and Beall, G. W. (2012) Direct growth of carbon nanotubes on hydroxyapatite using MPECVD Mater. *Chem. Phys.*, 132(1): 119–124.
- Beall, G. W., Duraia, E.-S. M. A., Yu, Q., and Liu, Z. (2014) Single crystalline graphene synthesized by thermal annealing of humic acid over copper foils. *Physica E*, 56: 331–336.
- Duraia, E.-S. M. A., Burkitbaev, M., Mohamedbakr, H., Mansurov, Z., and Beall, G. W. (2010) Growth of carbon nanotubes on diatomite. *Vacuum*, 84: 464–468.
- Duraia, E.-S. M. A., Mansurov, Z. A., and Tokmoldin, S. Zh. (2011) Formation of graphene by the thermal annealing of a graphite layer on silicon substrate in vacuum. *Vacuum*, 86(2): 232–234.
- Tauc J. (1974) *Amorphous and Liquid Semiconductors*. Plenum Press: New York.
- Aydin, C., Abd El-sadek, M. S., Zheng, K., Yahia, I. S., and Yakuphanoglu, F. (2013) Synthesis, diffused reflectance and electrical properties of nano-crystalline Fe-doped ZnO via sol-gel calcination technique. *Opt. Laser Technol.*, 48: 447–452.
- Martel, R., Schmidt, T., Shea, H. R., Hertel, T., and Avouris, Ph. (1998) Single- and multi-wall carbon nanotube field-effect transistors. *Appl. Phys. Lett.*, 73: 2447–2449.
- Yang, M., Kim, H. C., and Hong, S. H. (2012) DMMP gas sensing behavior of ZnO-coated single-wall carbon nanotube network sensors. *Mat. Lett.*, 89: 312–315.
- Kuo, C. Y. (2009) Preventive dye-degradation mechanisms using UV/TiO₂/carbon nanotubes process. *J. Hazard. Mater.*, 163: 239–244.
- Popov, V. N. (2004) Carbon nanotubes: Properties and application. *Mat. Sci. Eng. R*, 43: 61–102.
- Park, J. S., Lee, J. M., Hwang, S. K., Lee, S. H., and Lee, H. J. (2012) A ZnO/N-doped carbon nanotube nanocomposite charge transport layer for high performance optoelectronics. *J. Mater. Chem.*, 22: 12695–12700.
- Khurana, G., Sahoo, S., Barik, S. K., and Katiyar, R. S. (2013) Improved photovoltaic performance of dye sensitized solar cell using ZnO-graphene nano-composites. *J. Alloys Compd.*, 578: 257–260.
- Sarkar, S. and Das P. K. (2014) Role of interface on electrical conductivity of carbon nanotube/alumina nanocomposite. *Ceram. Int.*, 40: 2723–2729.
- Torrent, J. and Barron, V. (2002) *Encyclopedia of Surface and Colloid Science*. Marcel Dekker: New York.
- Morales, A. E., Mora, E. S., and Pal, U. (2007) Use of diffuse reflectance spectroscopy for optical characterization of un-supported nanostructures. *Rev. Mex. Fis.*, 53: 18–22.
- Senthilkumar, V., Vickraman, P., and Ravikumar, R. (2010) Synthesis of fluorine doped tin oxide nanoparticles by sol-gel technique and their characterization. *J. Sol-Gel Sci. Technol.*, 53: 316–321.
- Yakuphanoglu, F. (2010) Electrical characterization and device characterization of ZnO microring shaped films by sol-gel method. *J. Alloys Compd.*, 507: 184–189.
- Yakuphanoglu, F., Mehrotra, R., Gupta, A., and Munoz, M. (2009) Nanofiber organic semiconductors: The effects of nanosize on the electrical charge transport and optical properties of bulk polyanilines. *J. Appl. Polym. Sci.*, 114: 794–799.
- Caglar, M. and Yakuphanoglu, F. (2012) Structural and optical properties of copper doped ZnO films derived by sol-gel. *Appl. Surf. Sci.*, 258: 3039–3044.
- Serbetçi, Z., El-Nasser, H. M., and Yakuphanoglu, F. (2012) Photoluminescence and refractive index dispersion properties of ZnO nanofibers grown by sol-gel method. *Spectrochim. Acta A*, 86: 405–409.
- Mansour, Sh. A. and Yakuphanoglu, F. (2012) Electrical-optical properties of nano-fiber ZnO film grown by sol gel method and fabrication of ZnO/p-Si heterojunction. *Solid State Sci.*, 14: 121–126.